Next Materials 12 (2026) 102461

Contents lists available at ScienceDirect

Next Materials

journal homepage: www.sciencedirect.com/journal/next-materials

Research article

Influence of tungsten carbide reinforcement on the mechanical properties, fatigue life, and fracture morphology of kevlar/S2-Glass/epoxy hybrid laminates

Nilesh Sitaram Gaikwad [a,b], Dhiraj D. Deshmukh [a,*,1]

[a] MET's Institute of Engineering, Savitribai Phule Pune University, Pune, Maharashtra 411007, India
[b] Maratha Vidya Prasarak Samaj's KBTCOE, Nashik, Maharashtra 422013, India

ARTICLE INFO

Keywords:
Hybrid composites
Tungsten carbide
Mechanical properties
Fatigue behaviour
Fracture morphology
Defence laminates

ABSTRACT

Fiber-reinforced polymer composites (FRPCs) have gained considerable traction in high-performance engineering owing to their high specific strength, corrosion resistance, and tuneable mechanical behaviour, making them well-suited for lightweight structural and protective applications. Kevlar, an aramid fiber renowned for its elevated tensile strength, impact resistance, and energy-absorbing capacity, finds extensive use in ballistic and aerospace applications. S2-glass fibers, compared with conventional E-glass, offer superior rigidity, thermal stability, and fatigue endurance under high-stress service conditions. Tungsten carbide (WC), a hard ceramic particulate, acts as a secondary reinforcement capable of enhancing wear resistance and surface hardness without disproportionately increasing composite density. Contemporary hybrid composites incorporate multiphase reinforcements to achieve synergistic performance in defence-critical applications such as lightweight structural and protective components and vehicle structures; however, challenges related to interfacial toughness, delamination under cyclic loading, and production scalability persist. In the present study, seven hybrid laminates were fabricated via hot-press compression moulding incorporating varying WC content (0–20 wt%) within a Kevlar/S2-glass/epoxy matrix at a fixed resin fraction (35 wt%). Mechanical characterisation encompassed tensile, flexural, fatigue, and hardness tests, while microstructural and elemental distribution analyses were conducted using field-emission scanning electron microscopy (FESEM) and energy-dispersive X-ray spectroscopy (EDS). The unfilled hybrid laminate (32.5 wt% Kevlar and 32.5 wt% S2-glass) yielded the highest tensile strength of 268.62 MPa 52% and 273% greater than pure Kevlar and pure S2-glass laminates, respectively and the highest flexural strength of 365.81 MPa 88% and 138% greater than the respective baselines. While fatigue life under tension–tension cyclic loading (R = 0.1, 70% UTS) reached a maximum of 2335 cycles at 15 wt % WC approximately 10.6 times (957%) higher than pure Kevlar and approximately 292% above the unfilled hybrid baseline,beyond 15 wt%, WC particle agglomeration and micro-void formation degraded tensile ductility, as confirmed by EDS mapping. Tungsten distribution was homogeneous at 10–15 wt% WC, whereas pronounced particle clustering at 20 wt% correlated directly with the observed decline in tensile ductility and the associated reductions in fatigue life and flexural strength. Future investigations could explore nano-scale WC dispersions, optimized stacking sequences, and ballistic impact testing to further assess the potential of these hybrids for lightweight protective structures.

1. Introduction

Fiber-reinforced polymer matrix composites (PMCs) have emerged as leading candidates for high-performance structural and protective applications owing to their high specific strength, corrosion resistance, and tailorable mechanical properties [1,2]. Current developmental efforts concentrate on thick hybrid laminates capable of sustaining high-velocity impact, elevated temperature, and cyclic fatigue in operational environments [3,4]. Manufacturing is progressively transitioning toward scalable out-of-autoclave processing notably

* Corresponding author.
E-mail address: dhirgajanan@gmail.com (D.D. Deshmukh).
[1] ORCID ID: 0000-0001-8673-4520

https://doi.org/10.1016/j.nxmate.2026.102461
Received 27 April 2026; Received in revised form 29 May 2026; Accepted 7 June 2026
Available online 9 June 2026
2949-8228/

vacuum-assisted resin transfer moulding (VARTM) and automated fiber placement (AFP) to meet production demands [5]. Despite these advances, maintaining consistent fiber volume fraction, low porosity, and interlaminar homogeneity in large-format laminates remains a significant manufacturing challenge. Naik [6] demonstrated that matrix chemistry and interfacial adhesion control are critical determinants of ballistic performance and long-term durability under coupled loading conditions. Ravikumar et al. [7] reported that the addition of WC particles to AA6082 aluminium alloy improved hardness and tensile strength, while impact strength and ductility decreased with increasing reinforcement content. SEM analysis revealed both ductile and brittle fracture features due to strong interfacial bonding between WC particles and the aluminium matrix. Similarly, Shivashankar et al. [8] observed that hybrid reinforcement of graphite and WC significantly enhanced the tensile strength, yield strength, and hardness of Al6061 composites, with the 4% Gr–6% WC composition exhibiting the best mechanical performance.

Kevlar fibers (poly(p-phenylene terephthalamide)) serve as effective reinforcements in impact-resistant composites due to their high tensile strength (3.6–4.1 GPa), strain-to-failure (~3.5–4.0%), and capacity to dissipate fracture energy through fibrillation, splitting, and pull-out mechanisms [9,10]. Surface modification strategies including plasma treatment, polydopamine coating, and silane functionalization enhance fiber–matrix adhesion and improve interlaminar fracture toughness and mode-II delamination resistance of epoxy systems by 40–90% [9]. Toughened matrices incorporating rubber or thermoplastic interleaves (PEEK, PEI) suppress crack propagation and improve residual compressive strength following low-velocity impact [10]. Rezasefat et al. [11] demonstrated through experimentation and high-fidelity modelling that S2-glass woven fabric reinforced polymer composites exhibit dynamic behaviour and permanent indentation under impact, with response strongly governed by fabric architecture and resin properties. The hybridisation of Kevlar composites with stiffer reinforcements enhances tensile modulus and high-strain-rate performance. Nevertheless, Kevlar composites continue to exhibit limitations in compressive strength, transverse shear performance, and resistance to moisture-induced hydrolytic degradation under severe environmental conditions [12]. Compared with conventional E-glass, S2-glass fibers offer a higher tensile modulus, specific strength, softening point (>1050 °C), and fatigue endurance [13,14]. S2-glass/epoxy laminates retain more than 70% of their room-temperature flexural and interlaminar shear strength at temperatures up to 300 °C, enabling their application in engine nacelles, thermal protection systems, and high-temperature structural components [15]. Jankowiak [16] demonstrated low strain-rate sensitivity during high-velocity perforation, resulting in predictable and reproducible damage patterns under ballistic and blast loading a characteristic advantage over most carbon-fiber systems. Optimised machining parameters mitigate fiber pull-out, smearing, delamination, and thermal damage in thick S2-glass laminates [17]. Fire performance assessments indicate reduced heat release rates and lower smoke concentrations relative to conventional glass composites [18]. However, the large filament count and low crimp typical of S2-glass fabrics predispose thick laminates to resin-starved regions and elevated porosity [19]. Through-thickness reinforcements and modified vacuum-assisted infusion procedures are under active investigation to enhance interlaminar strength and dimensional reliability [20].

Hybrid Kevlar/S2-glass composites combine the toughness and energy-absorption characteristics of aramid fibers with the stiffness, fatigue endurance, and thermal stability of S2-glass, yielding a mechanical balance and damage tolerance superior to single-fiber systems [21,22]. Hygrothermal conditioning produced a 20–45% improvement in interlaminar shear strength and flexural rigidity compared with pure Kevlar laminates owing to reduced moisture ingress and enhanced interfacial compatibility [23]. Hosseini et al. [24] showed that S2-glass strike-face plies prevent back-face deformation under low-velocity impact while Kevlar core layers dissipate energy through delamination and fiber bridging. Complementary fiber interactions also minimise tribological contact stresses and suppress crack growth [25].

Fajdek-Bieda [26,27] reported improved tensile strength and flexural rigidity in optimised hybrid fiber composites. Ceramic particulates enhance hardness and wear resistance; Bak et al. [28] reviewed the phenomenology of delamination under fatigue loads and emphasised the importance of standardised test configurations and environmental control in fatigue testing of composite laminates. Hybrid Kevlar/glass reinforced epoxy/vinyl ester composites demonstrated improved tensile, flexural, and thermal performance owing to enhanced fibre–matrix interfacial bonding and reduced delamination [29]. Fatigue performance of fibre-reinforced composites can be substantially enhanced through incorporation of hybrid fillers and optimisation of reinforcement architecture and matrix systems [30].

Li et al. [31] demonstrated that aligned CNT–boron nitride networks improve thermal management and reduce CTE mismatch. Tran et al. [32] employed machine-learning models to predict decomposition behaviour, showing that phosphorus-based flame retardants can reduce peak heat release rates by 40–60%. Li et al. [33] emphasised the role of percolation thresholds and interface modification in achieving balanced thermal insulation in polymer-based thermally conductive composites. Vaze et al. [34] investigated the ballistic impact behaviour of carbon fiber and E-glass sandwiched composites, demonstrating progressive delamination with increasing backplate thickness under high-velocity projectile loading. Singh et al. [35] found that increased laminate thickness enhances energy absorption through greater delamination and fiber bridging, but also elevates interlaminar stresses at impact velocities exceeding 200 m/s. Biradar et al. [36] established that carbon/glass/Kevlar stacking sequences provided optimal load sharing, whereas asymmetric hybrids lost 30–50% residual strength owing to fiber kinking and matrix cracking. Junio et al. [37] reported that Kevlar/basalt hybrids exhibited improved low-velocity impact resistance attributable to enhanced inter-yarn friction, albeit with increased flammability at higher glass contents. Lei et al. [38] demonstrated that progressive damage models employing the Hashin criterion accurately predict fiber breakage and delamination, and that CAI (compression after impact) strength can be reduced by up to 40% in carbon/epoxy systems at elevated temperatures.

Multi-scale reinforcement strategies combining nanoparticles (graphene, CNTs, boron nitride), micro-ceramics, and hybrid fibers have emerged as effective means of simultaneously improving stiffness, fracture toughness, fatigue resistance, and multifunctional properties such as thermal conductivity and self-healing capability. Interfacial engineering through chemical functionalisation, plasma treatment, and hierarchical sizing significantly improves stress transfer and minimises filler agglomeration. Hamzat et al. [20] showed that fiber-reinforced composites for aerospace and marine applications are susceptible to failure under chemical, thermal, and mechanical loading, and that interfacial quality is a key determinant of long-term durability. Fang et al. [39] provided a comprehensive review of traditional and additive manufacturing processes for fiber-reinforced composites, highlighting how material architecture governs mechanical and thermal performance. Sustainable approaches including bio-derived epoxies and recycled fibers are increasingly adopted; Jeevan et al. [40] reviewed the performance and durability of natural and hybrid fiber-reinforced polymer composites and highlighted processing quality as a key determinant of mechanical performance. Kumar et al. [41] reported that recycled carbon fibers retained 85–95% of their original strength following optimised compression moulding. Kaya et al. [42] investigated the strain-rate and temperature-dependent behaviour of S2-glass/epoxy composites, revealing that elevated temperature substantially reduces static and dynamic strength. Farajyar et al. [43] conducted finite element analysis of ballistic impact on Kevlar−29/epoxy composites with varying layer configurations, while Worku et al. [44] identified poor compressive performance of Kevlar and limited S2-glass availability as persistent barriers, proposing surface treatment and process automation as mitigation strategies.

The latest investigations on the interfacial properties of tungsten carbide in metal and polymer composites have produced additional knowledge of their structures. Aghdasi et al. [45] studied the interface between iron, molybdenum-doped, and chromium-doped WC and found dopants increased interfacial adhesion. Aghdasi et al. [46] further analysed metal-substituted W_4C_4 carbides in cobalt and determined that this change in chemical bonding properties helps to improve interfacial stability through the use of the electronic structure. More recently Li [47] used the electron work function to characterise the interfacial bonding of doped WCs in nickel composite systems and provide additional information about improving the compatibility of these materials with polymer composites through the use of the interfacial characteristics. The data provided from these theoretical studies supports the finding of this present experimental study that shows benefits of well-dispersed WCs (10–15 wt%) on enhancing crack deflection and load transfer due to the presence of the epoxy matrix.

Proposed study fills an important void in the literature by producing and characterising seven types of hybrid laminate made from hot-pressed composite materials using Kevlar, S2 glass, tungsten carbide, and epoxy as the matrix materials. A combination of tensile (test and static), flexural (3-point bend), hardness and tension-tension fatigue properties were evaluated, and quantitative analyses using detailed FESEM fractography and EDS were provided to support the material performance data. Out of the seven developed laminate composites, all exhibited superior mechanical and fatigue performance for use in structural applications and/or protective applications; however, impact testing for ballistic performance was not performed as part of this research study. In addition, the investigational study has revealed important characterisation data regarding the microstructure-property relationship by interpreting the effects of varying the WC content on the properties of the composites produced. Finally, it has identified the optimal (10–15 wt%) composition of the WC for future development of lightweight/high-fidelity fatigue resistant composites, based on good static strength, hardness and endurance (fatigue) properties.

2. Materials, Fabrication, and Characterisation

2.1. Materials

Four constituent materials were employed in the fabrication of the hybrid composites: (i) Kevlar fabric (poly(p-phenylene terephthalamide)), (ii) S2-glass (magnesium aluminosilicate glass fiber) plain-weave fabric, (iii) tungsten carbide (WC) micro-powder, and (iv) a bisphenol-A epoxy matrix comprising ARALDITE LY 556 resin with HY 951 hardener. Kevlar and S2-glass plain-weave fabrics were procured from Fiber Source, Chennai, India. High hardness and wear-resistance properties were contributed by WC powder (94–97% purity, 1–3 μm particle size) sourced from Sigma-Aldrich, India. The epoxy system was supplied by Huntsman Solutions India Pvt. Ltd., Mumbai, India, and was selected for its low viscosity and excellent post-cure mechanical properties. Table 1 summarises the key material properties derived from supplier data sheets and standard characterisation.

It is worth noting that the concentrations of WC used, i.e. 0, 5, 10, 15, and 20 wt%, have been carefully selected from an extensive body of literature concerning ceramic particulate reinforcement in polymer composite materials, including initial dispersion tests performed in our lab. It is well known that previous studies of micro and nano-ceramic particles added into epoxy-based systems exhibited best mechanical properties when the filler weight fraction ranged between 5–15 wt%, above which significant agglomeration and an elevated resin viscosity usually occurred, resulting in inferior processing capabilities and interface properties [e.g., 25, 34, 36]. Initial trials demonstrated that dispersion of WC particles (size 1–3 μm) was possible up to 15 wt% by means of high shear mixing followed by ultrasonic treatment and degassing. In addition, at 20 wt% content a visible increase in viscosity and slight agglomeration occurred, which was purposefully introduced to define the upper threshold of reinforcement efficiency. Consequently, the proposed range allows obtaining a complete picture of WC concentration dependency regarding its influence on microstructure, mechanical properties, fatigue resistance, and fracture mechanics of the considered Kevlar/S_2 hybrid system.

2.2. Fabrication of Hybrid Composite Laminates

To ensure good reproducibility, 7 hybrid laminates were fabricated by hot-press, compression moulding technique. The primary reinforcements were bi-directional plain weave Kevlar 29 and S2-glass fabrics (200 g/m^2 areal density), and the epoxy resin (Araldite LY 556) and hardener (HY 951) had a fixed weight ratio of 100:10, which yielded a constant matrix content of 35 wt% in all compositions. Microparticles of tungsten carbide (WC) (1–3 μm, 94–97% purity) were added by proportionally decreasing the total fiber content as 0, 5, 10, 15 and 20 wt%. Fabrics were cut into 15 layers of 320 mm × 320 mm and layers were symmetrically stacked in a $[K/G]_7K$ sequence (K = Kevlar, G = S2-glass) for hybrid compositions. To minimize the agglomeration of the WC particles, they were dispersed in the epoxy resin using a high-shear mechanical stirrer at 2000 rpm for 30 min, and then ultrasonically treated (750 W, 20 kHz) for 45 min in an ice bath.

This mixture was then degassed under vacuum (–0.8 bar) for 20 min. The hardener was then added and mixed lightly for 5 min and then wet hand lay-up was carried out. The stacked preforms were sandwiched between steel plates coated with a release material in a 1 tonne hydraulic hot press. The curing was done in two steps: initial curing at room temperature under 3 MPa for 15 min, followed by post curing at 50 °C under 3 MPa for 60 min, and controlled cooling at 2 °C/min to room temperature. The resulting panels were all uniformly sized (300 mm × 300 mm) with a nominal thickness of 3.1 ± 0.3 mm, a void content of less than 2.5%, and a fiber volume fraction (fVF) between 62–66%. To guarantee the reproducibility of all laminates, they were manufactured under the same conditions. The details of the compositions of each laminate are given in Table 2.

The fiber volume fraction (Vf) and void content of the cured laminates was determined by the ignition (burn-off) method as per ASTM D3171, Procedure A. Accurately weighed rectangular specimens (25 mm × 25 mm) were cut from various parts of each panel and then ignited at high temperature under 590 ± 10 °C for 4 h in a muffle furnace

Table 1
Physical and mechanical properties of raw materials used in hybrid composite fabrication. †WC value in the Flexural/Transverse Rupture Strength column represents transverse rupture strength (TRS), not uniaxial tensile strength.

Material	Density (g/cm^3)	Flexural/Transverse Rupture Strength (GPa)	Modulus (GPa)	Elongation (%)	Notable Properties
Kevlar Fabric	1.44	3.6	112	3.5	Areal wt. 220 g/m^2; thickness 0.3 mm; Mohs hardness N/A
S2-Glass Fabric	2.46	4.8	86.8	5.4	Areal wt. 220 g/m^2; thickness 0.3 mm; softening pt. > 1050 °C
Tungsten Carbide (WC)	15.6	†5–7	530–700	—	†TRS (transverse rupture strength); Mohs 9; CTE 5.0–5.5 × 10^{-6}/°C; particle size 1–3 μm
Epoxy (LY556/HY951)	1.15–1.20	—	—	—	Viscosity 10,000–12,000 mPa·s at 25 °C; Tg ≈ 140–150 °C; CTE 60–70 × 10^{-6}/°C

Table 2
Constituent composition (wt%) of the fabricated hybrid composite laminates.

Sample Code	Kevlar (wt%)	S2-Glass (wt%)	WC (wt%)	Epoxy (wt%)
NKEVLAR	65	0	0	35
NSGLASS	0	65	0	35
HKSGC1	32.5	32.5	0	35
HKSGC2	30	30	5	35
HKSGC3	27.5	27.5	10	35
HKSGC4	25	25	15	35
HKSGC5	22.5	22.5	20	35

NKEVLAR: neat Kevlar baseline; NSGLASS: neat S2-glass baseline; HKSGC: Hybrid Kevlar S2-Glass Composite.

to completely burn off the epoxy matrix. The weight of the residual fiber was measured and the fiber volume fraction was calculated by using the known densities of Kevlar, S2-glass, WC and epoxy. Five samples were tested for each laminate composition. The measured fiber volume fraction values were found to be in the range of 62–66% and the void content is always less than 2.5%, which means good consolidation quality in all the compositions.

2.3. Characterisation Methods

Mechanical and microstructural characterisation of the hybrid Kevlar/S2-glass/WC/epoxy laminates was performed in accordance with established ASTM standards. Tensile testing was conducted on an

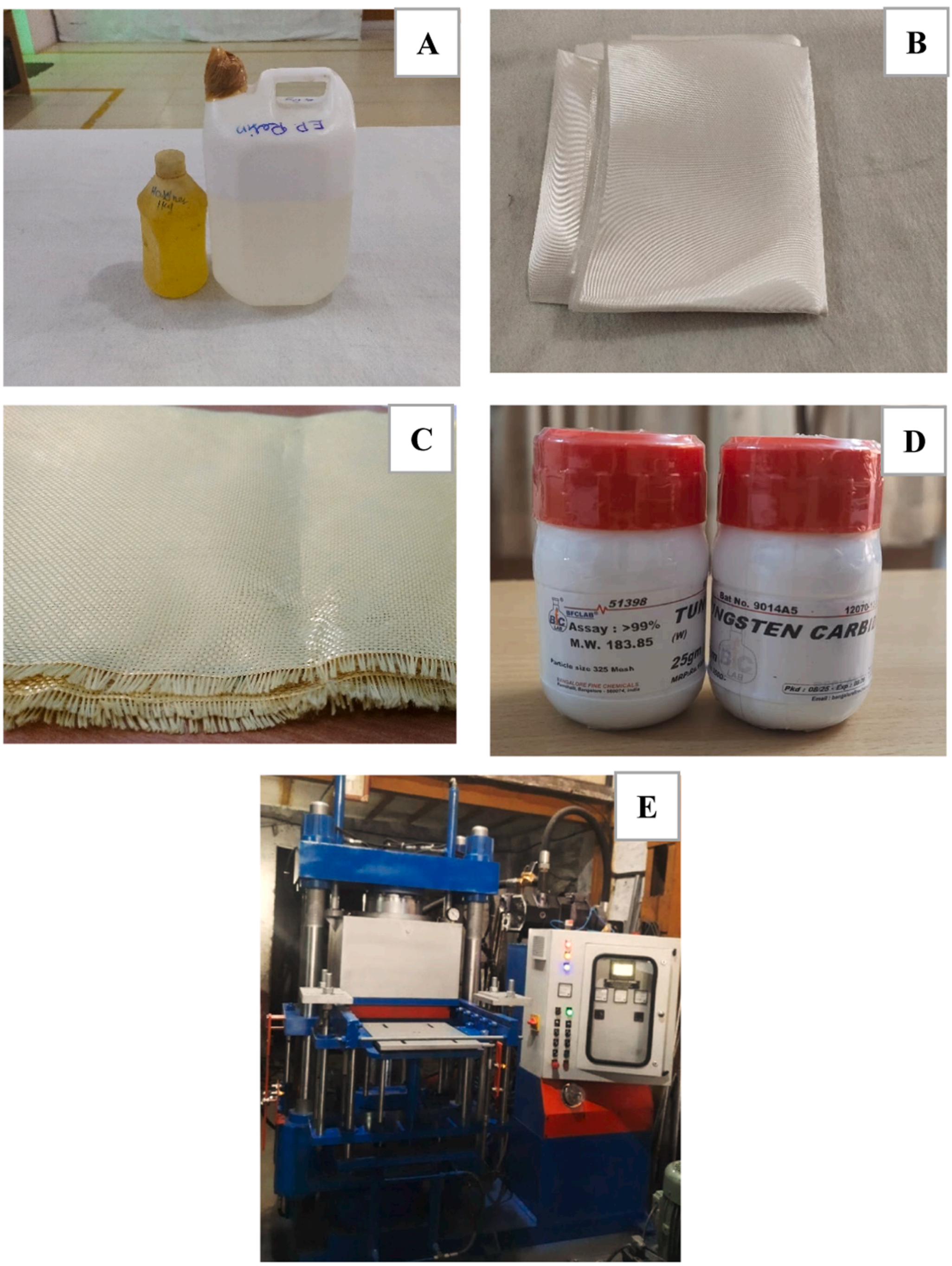

Fig. 1. Constituent raw materials and fabrication equipment: (A) Araldite LY 556 epoxy resin and HY 951 hardener; (B) S2-glass plain-weave fabric; (C) Kevlar 29 plain-weave fabric; (D) tungsten carbide micro-powder; (E) hot-press compression moulding system.

Instron 8801 universal testing machine (100 kN capacity) per ASTM D3039, using five replicate specimens (250 × 25 × 3 mm, gauge length 150 mm) at a crosshead displacement rate of 2 mm/min, yielding tensile strength, tensile modulus, elongation at break, and characteristic failure modes including fiber pull-out and matrix cracking. Flexural properties were determined via three-point bending per ASTM D7264 on the same machine, with specimens of dimensions 100 × 13 × 3 mm and a span of 60 mm at 2 mm/min; five replicates were tested to obtain flexural strength, flexural modulus, and flexural strain. The fatigue behaviour was investigated under tension–tension cyclic loading (stress ratio R = 0.1, frequency 5 Hz) at a constant maximum stress level of 70% of the respective ultimate tensile strength (UTS) as per ASTM D3479. The relative high cycle fatigue performance of the laminates was compared by testing five replicate specimens for each composition and recording the number of cycles to failure. Surface hardness was measured using a Shore D durometer per ASTM D2240 on polished specimens (50 × 50 × 3 mm); the reported value represents the mean of ten indentations per specimen, used to correlate surface resistance with WC content. Fracture surfaces and undeformed cross-sections were examined by FESEM (ZEISS, 5–15 kV) at magnifications up to 5000 × , following gold sputter-coating of specimens. Elemental composition and spatial distribution of constituent elements (C, O, Si, Mg, W) were determined by EDS coupled with FESEM to assess WC dispersion homogeneity and fiber–matrix interfacial integrity across all compositions.

3. Results and Discussion

3.1. FESEM Morphology of Undeformed Surfaces

FESEM examination of undeformed laminate surfaces (Fig. 2)

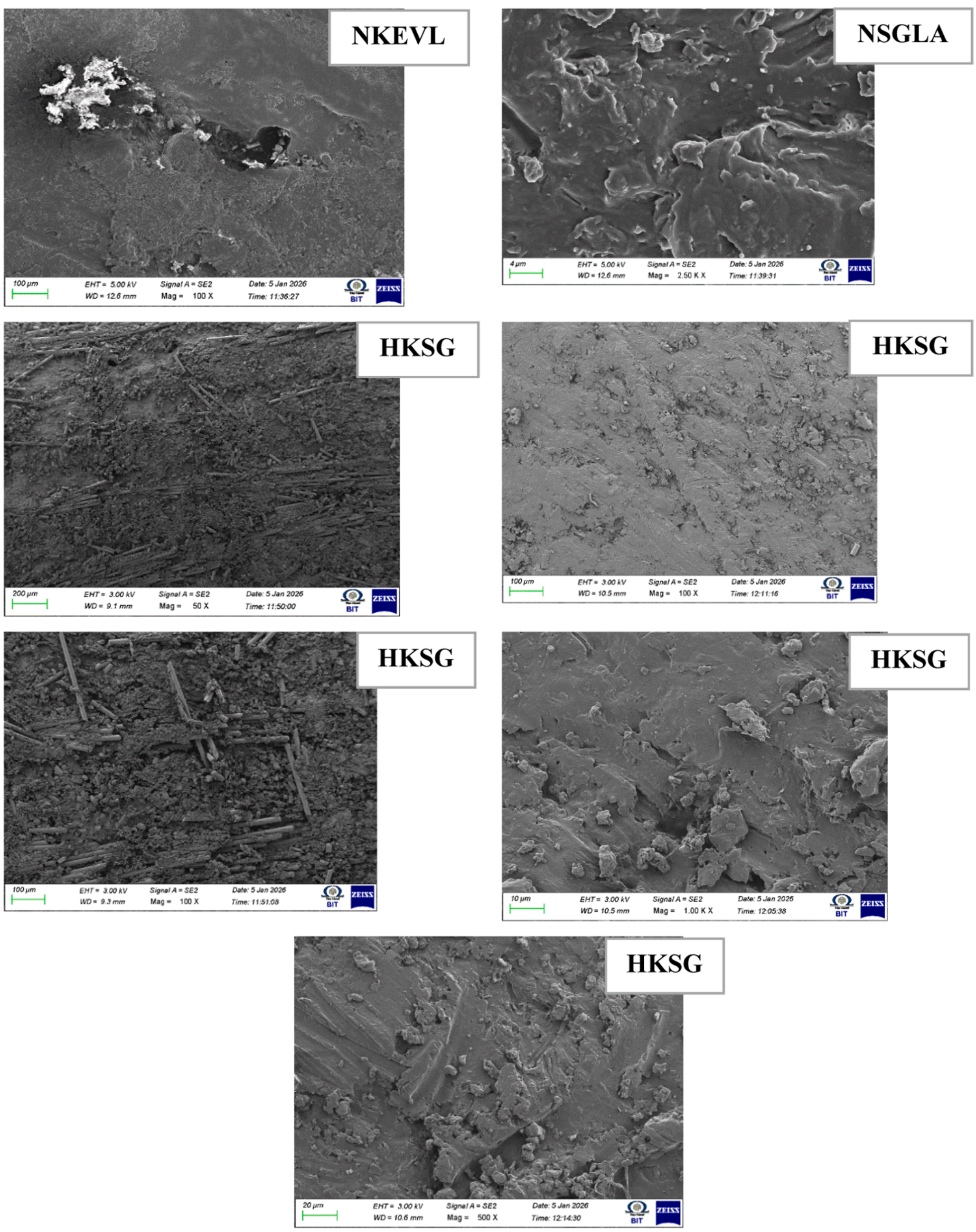

Fig. 2. FESEM surface morphology of undeformed hybrid composite laminates at representative magnifications: (a) NKEVLAR, (b) NSGLASS, (c) HKSGC1, (d) HKSGC2, (e) HKSGC3, (f) HKSGC4, (g) HKSGC5.

revealed distinct surface morphologies as a function of fiber type and WC content. The pure Kevlar laminate (NKEVLAR) exhibited a relatively smooth surface with occasional resin pockets and small voids (~50–100 μm), indicative of adequate but incomplete fiber wetting. The pure S2-glass laminate (NSGLASS) displayed a homogeneous wave-like topography with clearly defined fiber impressions and well-impregnated resin, consistent with the higher filament count and resin compatibility of S2-glass. The unfilled hybrid (HKSGC1) presented the most complex surface texture, with evenly distributed protruding fibers and well-defined interlaminar interfaces, confirming effective load transfer and fiber intermingling at 0 wt% WC with 35 wt% epoxy under hot-press processing conditions.

Progressive incorporation of WC micro-particles produced increasingly heterogeneous surface morphologies. At 5 wt% WC (HKSGC2), particles appeared as finely dispersed bright specks (~1–3 μm) distributed uniformly around the fibers with minimal clustering. The particle density increased at 10 wt% WC (HKSGC3), with the majority of particles remaining well dispersed, although small clusters (~5–8 μm) were identified at fiber crossover points. At higher WC loadings, dispersion quality deteriorated markedly: the 15 wt% laminate (HKSGC4) exhibited distinct agglomerates in the 10–20 μm size range, while the 20 wt% laminate (HKSGC5) contained large particle clusters exceeding 30 μm, accompanied by incompletely wetted fibers. These findings indicate that WC loadings above 10 wt% exceed the dispersibility threshold of the adopted mixing protocol, increasing resin viscosity and promoting void formation. In summary, unfilled and low-WC (≤10 wt%) laminates demonstrated superior fiber wettability and microstructural homogeneity, whereas higher WC content introduced defects that are expected to impair mechanical and fatigue performance.

Using Image J software, the size of WC particle agglomerates was evaluated quantitatively. For each composition, at least fifty randomly-selected agglomerates from eight to ten high-magnification FESEM pictures (magnification=500x–2000x) were measured. The average size is reported as the equivalent circular diameter. The majority of the agglomerates at 15 wt% WC laminate (HKSGC4) were between 10 and 20 μm (mean=14.8 ± 3.6 μm). At 20 wt% WC (HKSGC5) significantly larger clusters of WC agglomerates were found (ranging from 25 to 45 μm average diameter=32.7 ± 6.9 μm). Quantitative data also confirms that the tendency for the agglomeration of WC particles increased suddenly at or beyond 15 wt% WC correlating directly with a decline in mechanical strength and an increase in the number of voids created during the experimental process.

3.2. Tensile Properties

The tensile strength of the hybrid laminates was strongly influenced by fiber hybridisation and WC content (Fig. 3). The pure S2-glass laminate (NSGLASS) recorded the lowest tensile strength of 71.93 MPa, attributed to its inherently brittle fracture mode and limited energy absorption capacity. The pure Kevlar laminate (NKEVLAR) attained 176.96 MPa, benefiting from fiber strain capacity and fibrillation-mediated energy dissipation. The unfilled hybrid laminate HKSGC1 (32.5 wt% Kevlar + 32.5 wt% S2-glass) yielded the highest tensile strength of 268.62 MPa 51.8% and 273% greater than pure Kevlar and pure S2-glass, respectively demonstrating a pronounced positive hybrid effect attributable to load redistribution from the stiffer S2-glass plies to the ductile Kevlar layers, thereby delaying delamination onset through fiber bridging.

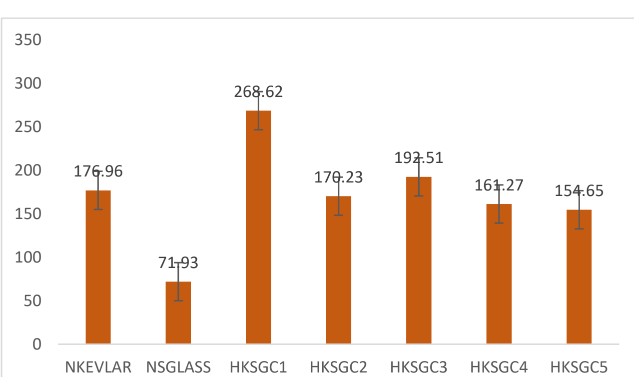

Fig. 3. Tensile strength of hybrid composite laminates as a function of WC content. Error bars represent one standard deviation (n = 5).

The addition of WC led to a non-linear change in tensile strength. Incorporation of 5 wt% WC (HKSGC2) reduced tensile strength to 179.23 MPa near that of pure Kevlar attributable to the reduction in total fiber content and the introduction of particle–matrix interface defects at this stage of loading. This was followed by a slight improvement to 192.51 MPa for 10 wt% of WC (sample HKSGC3). The tensile strength dropped to 161.27 MPa and 154.65 MPa upon increasing to 15 wt% and 20 wt%. At elevated loadings (15–20 wt%), particle agglomeration, micro-void formation, and weakened particle–matrix interfaces introduce stress concentrations that promote premature matrix cracking and interfacial debonding, as evidenced in FESEM fractographs (Section 3.5), thereby reducing the effective load-bearing cross-section and promoting brittle fracture. Tensile modulus followed a comparable trend, with HKSGC1 exhibiting peak rigidity attributable to the balanced contribution of S2-glass stiffness and Kevlar toughness. Overall, the unfilled hybrid laminate offers optimal tensile performance; moderate WC addition (≤10 wt%) is permissible when enhanced hardness and wear resistance are required, provided that adequate dispersion quality is maintained.

However, it should be noted that the increase of the WC particle amount was carried out at a proportional decrease of the total weight of the Kevlar and S2-glass fibers, maintaining constant the same percentage of the epoxy matrix (35 wt%). Therefore, the changes of mechanical properties were caused by a complex effect of WC reinforcement and fiber decrease. In order to differentiate between these two contributions, the hybrid laminate without any fillers (HKSGC1, 65 wt% total fiber) was used for studying the contribution of WC particles addition. The significant decrease of tensile and bending strength after reaching values between 10–15 wt% of WC particles, considering the reinforcement nature of ceramic particles, demonstrates convincingly that the negative contribution of fiber removal and agglomeration is stronger than reinforcement. It is confirmed by the FESEM and EDS analysis showing an increase of agglomeration and micropores appearance for values above 15–20 wt% WC.

3.3. Fatigue Behaviour

A marked improvement of the tension–tension fatigue performance (R = 0.1, 5 Hz, at constant stress level of 70% UTS) was observed with both fiber hybridisation and WC incorporation (Fig. 4). The pure Kevlar laminate (NKEVLAR) failed at 221 cycles and the pure S2-glass laminate (NSGLASS) at 312 cycles, reflecting rapid damage accumulation in the single-fiber systems. The unfilled hybrid HKSGC1 achieved 595 cycles 170% and 91% greater than pure Kevlar and S2-glass, respectively owing to the capacity of Kevlar layers to bridge and arrest cracks originating in the more brittle S2-glass plies. Incorporation of WC further and substantially extended fatigue resistance: 1962 cycles at 5 wt% (HKSGC2), 2106 cycles at 10 wt% (HKSGC3), and a maximum of 2335 cycles at 15 wt% (HKSGC4). The slight reduction to 2284 cycles at 20 wt % WC (HKSGC5) remained significantly above the unfilled hybrid baseline. At 15 wt% WC, fatigue life was enhanced by approximately 957% (approximately 10.6 ×) relative to pure Kevlar and approximately 292% relative to the unfilled hybrid.

The improvements in fatigue life are attributable to crack deflection, crack pinning, and energy dissipation mechanisms activated by well-dispersed WC particles within the epoxy matrix. At optimum WC

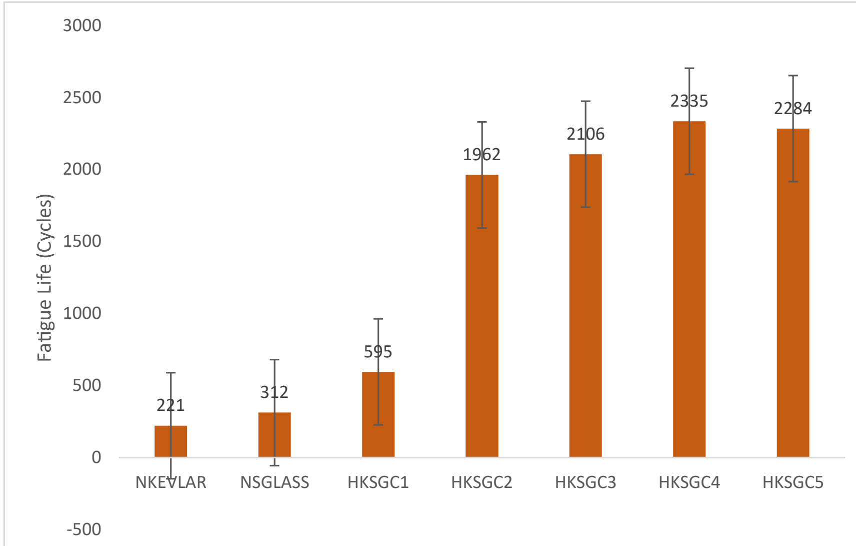

Fig. 4. Fatigue life of hybrid composite laminates under tension–tension loading (R = 0.1, 70% UTS).

loadings (10–15 wt%), particles impose tortuous crack propagation paths, increasing the effective crack surface area and consuming energy through matrix deformation and particle–matrix interfacial debonding. This mechanism is further amplified by the hybrid architecture: strain concentration in stiff S2-glass plies is moderated by ductile Kevlar layers that dissipate energy via fibrillation and pull-out, creating a damage-tolerant load-sharing system. The marginal reduction in fatigue life at 20 wt% WC is consistent with FESEM morphological evidence of agglomeration and micro-voids that facilitate premature crack nucleation. At 15 wt% WC, fatigue life was enhanced by approximately 957% (approximately 10.6 ×) relative to pure Kevlar and approximately 292% relative to the unfilled hybrid. However, it is important to mention that the fatigue test was performed at only one level of stress (70% of ultimate tensile strength). In order to obtain a full S-N diagram, it is necessary to perform tests at several different levels of stress.

3.4. Flexural Properties

Flexural behaviour under three-point bending (ASTM D7264) followed trends broadly consistent with tensile performance, confirming the dominant roles of fiber hybridisation and WC content (Fig. 5). The pure S2-glass laminate (NSGLASS) exhibited the lowest flexural strength of 153.82 MPa owing to brittle compressive face-sheet failure and limited interlaminar shear resistance. Pure Kevlar (NKEVLAR) reached 194.97 MPa by virtue of its superior strain-to-failure. The unfilled hybrid HKSGC1 achieved the highest flexural strength of 365.81 MPa 87.6% and 138% greater than pure Kevlar and S2-glass, respectively with S2-glass outer plies resisting bending stresses efficiently and inner Kevlar layers retarding delamination through fiber bridging and pull-out.

WC addition produced a non-monotonic flexural response: strength decreased to 167.06 MPa at 5 wt% (HKSGC2), recovered to 230.88 MPa at 10 wt% (HKSGC3), peaked marginally at 235.27 MPa at 15 wt% (HKSGC4), and declined to 179.64 MPa at 20 wt% (HKSGC5). At moderate loadings (10–15 wt%), well-dispersed WC particles augment matrix modulus and pin interlaminar cracks, delaying delamination and increasing bending stiffness. The marginal superiority of HKSGC4 over HKSGC3 in flexure despite similar tensile behaviour suggests that ceramic inclusions provide additional resistance when compressive, tensile, and interlaminar shear stresses act simultaneously in three-point

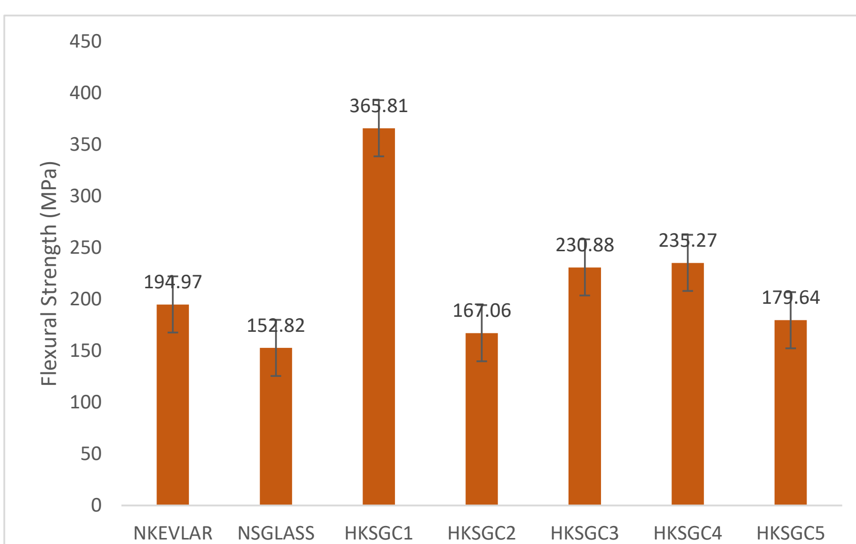

Fig. 5. Flexural strength of hybrid composite laminates under three-point bending (ASTM D7264).

bending. At 20 wt% WC, agglomeration-induced stress concentrations and micro-voids promote premature compressive-face cracking and accelerated interlaminar failure, reducing flexural strength below the pure Kevlar baseline. While the unfilled hybrid retains the highest absolute flexural strength, the 15 wt% WC laminate (HKSGC4) represents a favourable compromise when simultaneous improvements in hardness and wear resistance are required an important attribute for bending-critical defence components such as vehicle floor panels, helmet shells, and structural armour.

3.5. Shore D Hardness

Shore D hardness values exhibited a non-monotonic dependence on WC content (Fig. 6). The pure S2-glass laminate (NSGLASS) recorded the lowest hardness (78.8 Shore D) owing to higher surface resin content and softer fiber-face morphology, while the pure Kevlar laminate (NKEVLAR) registered a marginally higher value of 79.6 attributed to denser fiber packing. The unfilled hybrid (HKSGC1) advanced to 80.8, reflecting improved surface rigidity from balanced fiber packing. Hardness peaked at 81.6 Shore D for the 10 wt% WC laminate (HKSGC3) 2.0 units above the unfilled hybrid and 3.0 units above pure S2-glass and declined at higher loadings: 78.4 at 5 wt% (HKSGC2), 79.4 at 15 wt% (HKSGC4), and 78.0 at 20 wt% (HKSGC5).

The anomalous decrease at 5 wt% WC is attributable to insufficient particle density to produce measurable surface reinforcement. The subsequent peak at 10 wt% reflects a critical particle packing density at which well-dispersed, high-hardness WC inclusions (Vickers hardness 2600–3000 HV) maximise matrix stiffening and load-bearing capacity. The declining hardness at 15–20 wt% WC is consistent with the FESEM evidence of agglomeration (Fig. 2), wherein particle clusters create resin-rich micro-regions and micro-voids that lower resistance to indentation. Accordingly, 10 wt% WC (HKSGC3) represents the optimal composition for maximising surface hardness and abrasion resistance. This laminate also offers a favourable combination of hardness (81.6 Shore D), fatigue life (2106 cycles), and flexural strength (230.88 MPa), making it the preferred candidate for wear-critical defence components such as underbody panels, helmet shells, and surfaces subjected to repeated impact or abrasion.

3.6. Fracture Morphology

FESEM examination of fracture surfaces obtained from tensile, flexural, and fatigue specimens (Fig. 7) revealed distinctly different failure modes as a function of WC content, consistent with the observed mechanical trends. In the unfilled hybrid (HKSGC1) and low-WC laminates (HKSGC2 and HKSGC3), the dominant fractographic features were extensive Kevlar fiber pull-out (Figs. 7a–7c), pronounced fibrillation and longitudinal splitting of Kevlar filaments, and ductile matrix deformation around S2-glass fibers. These characteristics indicate strong fiber–matrix adhesion and efficient stress transfer, enabling Kevlar layers to bridge and arrest cracks propagating through the stiffer S2-glass plies. River-line patterns on fiber surfaces and residual matrix debris on fiber pullout channels confirm energy dissipation through plastic deformation of the epoxy phase. In contrast, high-WC laminates (HKSGC4 and HKSGC5) exhibited reduced pull-out lengths, fiber fracture in preference to pull-out, and brittle matrix cleavage (Fig. 7d), consistent with the decline in tensile and flexural strength at elevated WC loadings. At 20 wt % WC, large agglomerates visible on the fracture plane acted as pre-existing crack initiation sites, promoting premature interfacial failure at the particle–matrix boundary.

At optimal WC loadings (10–15 wt%, HKSGC3 and HKSGC4), well-dispersed particles were firmly embedded within the epoxy, acting as crack-deflection sites and nucleating secondary microcracks (Fig. 7f). This tortuous crack-path geometry substantially increases crack propagation energy, consistent with the observed peak fatigue life (2106–2335 cycles) and elevated flexural strength in these compositions. Localised matrix deformation around individual particles further contributes to energy dissipation. At 20 wt% WC, severe agglomeration produced large clusters that debonded from the matrix, generating voids and acting as stress concentrators. These defects reduced the effective load-bearing cross-section and facilitated premature crack coalescence, directly explaining the concurrent reduction in tensile and flexural strength. Taken together, the fractographic evidence confirms that 10–15 wt% WC provides an optimal balance of interfacial bonding quality, crack-pinning effectiveness, and hybrid-fiber toughening, while WC contents exceeding 15 wt% introduce detrimental defects that degrade both static and fatigue performance. These observations corroborate the mechanical test data and underscore the critical importance of dispersion quality control in ceramic-filled polymer hybrid composites.

3.7. EDS Elemental Analysis

Energy-dispersive X-ray spectroscopy (EDS) coupled with FESEM

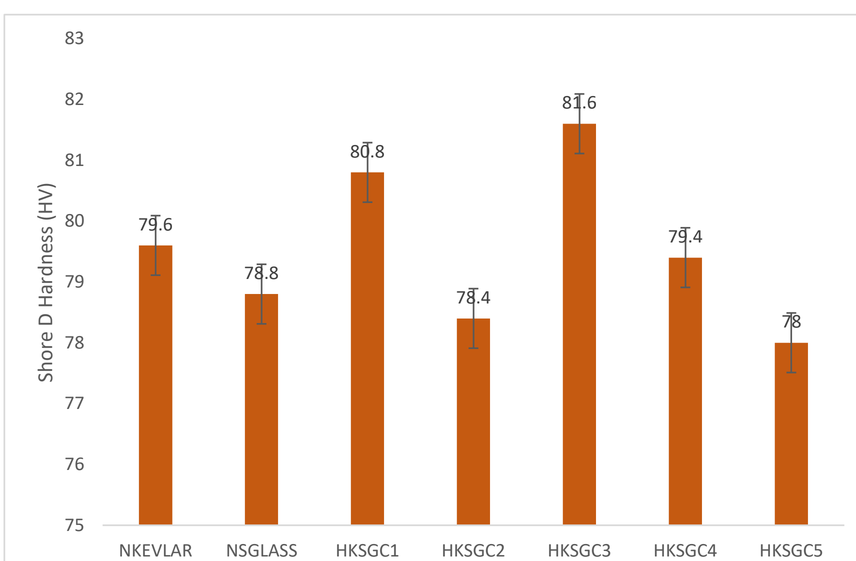

Fig. 6. Shore D hardness of hybrid composite laminates as a function of WC content.

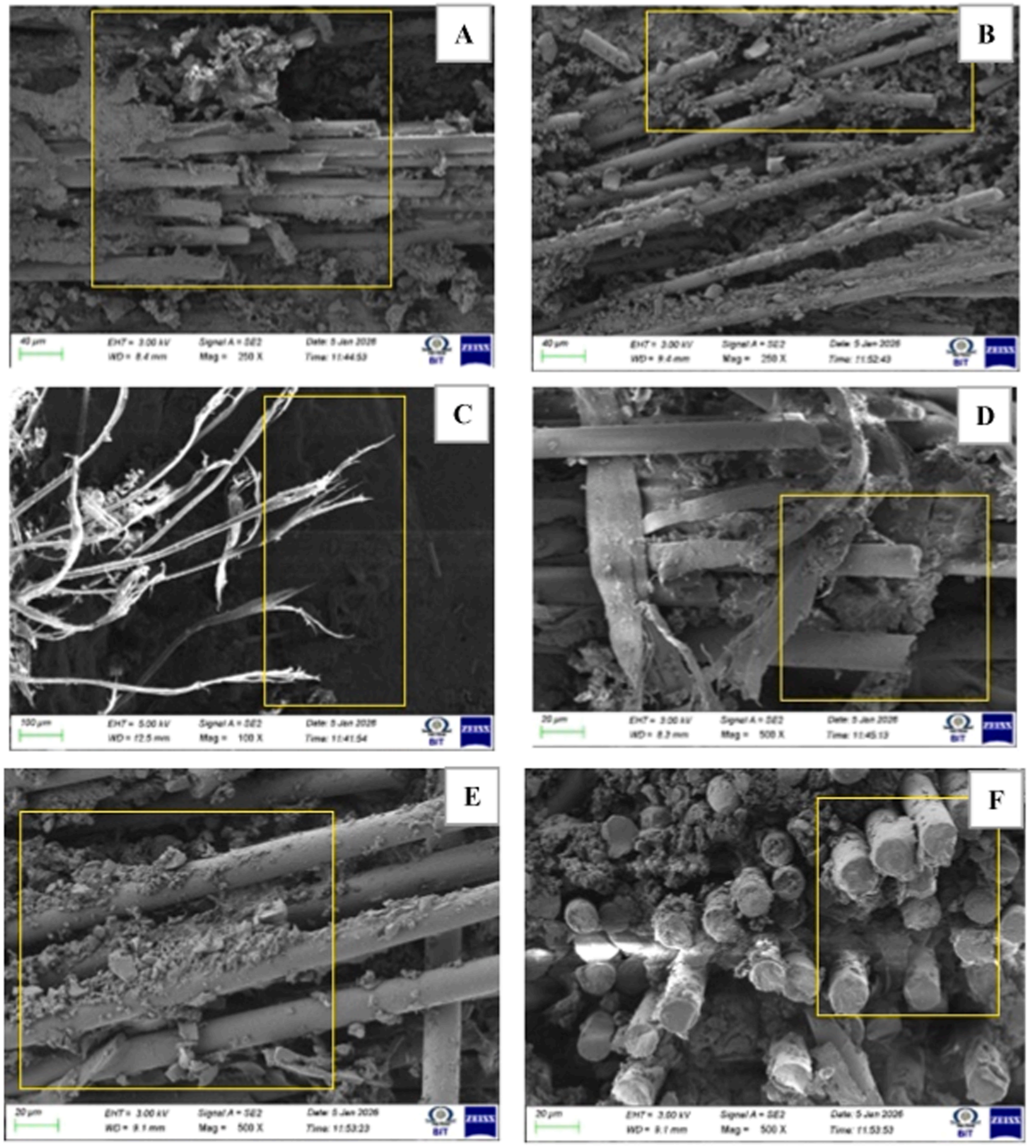

Fig. 7. FESEM fractographs of hybrid composite laminates following mechanical testing: (a) NKEVLAR, (b) NSGLASS, (c) HKSGC1 showing extensive fiber pull-out and fibrillation, (d) HKSGC5 showing brittle matrix cleavage and agglomerate-initiated fracture, (e) HKSGC3 showing river-line crack patterns, (f) HKSGC4 showing crack-deflection and pinning by WC particles.

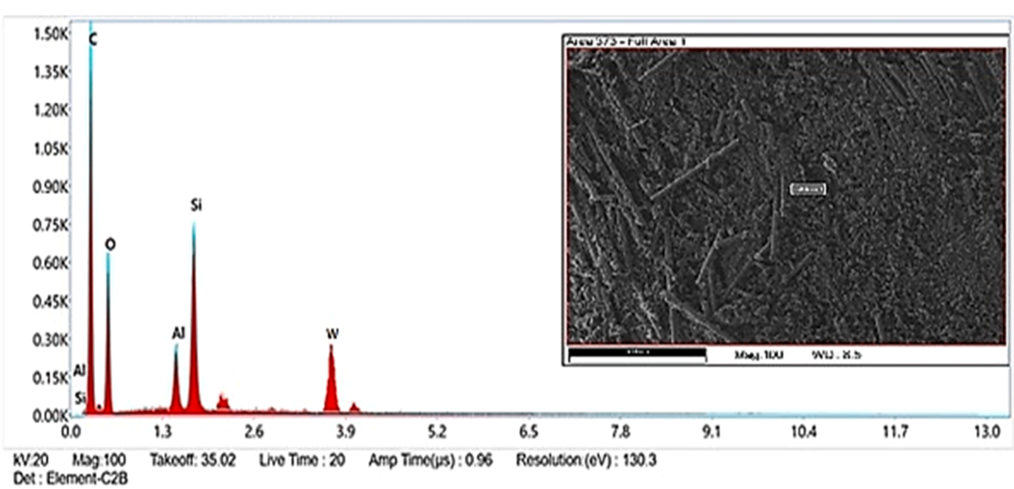

Fig. 8. EDS elemental analysis and mapping confirming WC distribution in hybrid composite laminates.

(Fig. 8) confirmed the elemental composition of the fracture surfaces and provided quantitative evidence of WC dispersion across all laminate compositions. In representative analysis areas, carbon (~69–76 wt%) and oxygen (~21–26 wt%) dominated the elemental spectrum, consistent with the bisphenol-A epoxy matrix. Silicon (~1.6–3.5 wt%) and aluminium (~0.6–1.3 wt%) signals confirmed the presence of aluminosilicate S2-glass fibers. The absence of a tungsten signal in fiber–matrix interface regions of the unfilled and low-WC laminates confirmed localised particle distribution and precluded preferential segregation of WC at the fiber–matrix interphase.

Elemental mapping of sections from the 10–15 wt% WC laminates (HKSGC3 and HKSGC4) revealed a spatially homogeneous tungsten distribution with minimal overlap with matrix-derived elements, confirming good interfacial compatibility and effective dispersion at these loadings. By contrast, the 20 wt% WC laminate (HKSGC5) exhibited localised high-intensity tungsten clusters concentrated around microvoids and exposed fibers, corroborating FESEM observations of particle agglomeration and directly correlating with the mechanical property deterioration documented in Sections 3.2–3.4. Taken together, the EDS findings affirm that controlled WC incorporation at 10–15 wt% yields a homogeneous reinforcement distribution that sustains effective crack deflection and energy absorption while preserving the structural integrity of the Kevlar/S2-glass hybrid architecture.

3.8. Statistical Analysis and Data Variability

The results of all mechanical tests conducted for each laminate composition were recorded as average values ± 1 standard deviation. Throughout this report, error bars displaying standard deviations were used in Figs. 3–6. The statistical significance between the various laminate compositions was determined using one-way analysis of variance (ANOVA) and Tukey's post-hoc at levels of $p < 0.05$. When comparing tensile and flexural strength properties, the data from laminates having no fillers (i.e. HKSGC1) compared to all other laminate compositions demonstrated a statistically significant difference ($p < 0.05$). The fatigue life for the laminate containing 15 wt% WC (i.e. HKSGC4) presented a statistically significant difference indicating that it had a statistically higher fatigue life compared to both the laminate with no fillers and laminates with WC content less than 15 wt% ($p < 0.05$). The hardness values of the laminate containing 10 wt% WC demonstrated a statistically significant difference from both the laminate with no fillers and laminates with WC levels greater than 10 wt% ($p < 0.05$). Additionally, the relatively low degree of variation (standard deviations were typically <8% for tensile/flexural strength and <12% for fatigue life) suggests that the fabrication and testing procedures were capable of producing repeatable results. The statistical analysis of these data indicates that the improvements in laminate properties observed for optimal incorporation of WC at loading levels between 10 and 15 wt% are statistically significant and cannot be attributed to variability in the experimental procedures.

3.9. Trade-off Between Mechanical Properties and Limitations of this study

The use of tungsten carbide (WC) in the Kevlar/S2-glass/epoxy hybrid system indicates obvious compromise between the properties investigated. The unfilled hybrid laminate (HKSGC1) showed the highest tensile strength (268.62 MPa) and flexural strength (365.81 MPa) among all the other samples, making it the optimum material when the static load bearing capacity is the main criterion. The fatigue life (595 cycles) and hardness (80.8 Shore D) were fairly low, however. WC particles were added to improve the fatigue life and hardness at the sacrifice of static strength. The 15 wt% WC laminate (HKSGC4) also had the highest fatigue life (2335 cycles) and good hardness (79.4 Shore D) but had 40% reduction in tensile strength and 36% reduction in flexural strength compared to the unfilled hybrid. The 10 wt% WC laminate (HKSGC3) had the highest hardness (81.6 Shore D), the longest fatigue life (2106 cycles) and had tensile (192.51 MPa) and flexural strength (230.88 MPa) that were acceptable. This trade off is governed mainly by the conflicting effects of WC reinforcement and fiber replacement. Crack deflection (which is beneficial for fatigue behavior) and matrix stiffness (which is beneficial for hardness behavior) are improved with well-dispersed WC particles, whereas excessive replacement of high-strength fibers and particle agglomeration at high loadings will reduce the tensile and flexural performance. For this reason, the best composition is dependent on the application: HKSGC1: High static strength, HKSGC3: High hardness with good static strength, and HKSGC4: High fatigue resistance with good static strength.

Although the present study gives a good understanding of mechanical and microstructural response of Kevlar/S2-glass/WC/epoxy hybrid composite, the following limitations of the study should be recognized. First, fatigue testing was only carried out at one high level of stress (i.e. 70% UTS) that does not allow the development of a complete S–N curve and therefore limited the understanding of fatigue at different levels of stress. Secondly the addition of WC was achieved by partial substitution of an equivalent weight fraction of reinforcing fibers and it is difficult to completely separate out the intrinsic effect of adding WC from the decrease in total fiber content. Third, there were no ballistic impact, low velocity impact or "moisture, UV, thermal cycling" tests performed and actual performance during real service conditions has not been verified. Last, the dispersion quality and interfacial bonding of micro scale WC particles were investigated, but those of nano scale WC particles or surface-treated particles were not investigated. These limitations will be worked on in the future to further validate the potential application of these hybrid composites.

4. Conclusions

In this work, seven Kevlar/S2-glass/tungsten carbide/epoxy hybrid laminates were successfully fabricated via hot-press compression moulding and systematically characterised for mechanical and microstructural properties as a function of WC content (0–20 wt%). The following principal conclusions are drawn.

1. The unfilled hybrid laminate (HKSGC1) exhibited the highest tensile strength (268.62 MPa) and flexural strength (365.81 MPa), demonstrating a pronounced positive hybrid effect 51.8% and 87.6% superior to pure Kevlar, and 273% and 138% superior to pure S2-glass in tension and flexure, respectively attributable to synergistic load redistribution between the stiffer S2-glass and more ductile Kevlar plies.
2. The fatigue life and surface hardness were substantially enhanced by WC incorporation, with optimal performance observed at 10–15 wt % WC. The 15 wt% WC laminate (HKSGC4) achieved the highest fatigue life of 2335 cycles under tension–tension loading at 70% UTS ($R = 0.1$), representing approximately 10.6 × (957%) the endurance of pure Kevlar and 292% above the unfilled hybrid baseline.
3. The 10 wt% WC laminate (HKSGC3) exhibited the maximum Shore D hardness (81.6), combined with good tensile (192.51 MPa) and flexural (230.88 MPa) strength, making it the preferred composition for wear-critical applications.
4. FESEM and EDS analyses confirmed that WC loadings of 10–15 wt% yield homogeneous particle dispersion, effective crack deflection, and crack pinning within the epoxy matrix, whereas loadings at 20 wt% cause pronounced particle agglomeration (mean cluster diameter 32.7 ± 6.9 μm) and micro-void formation, directly reducing tensile and flexural performance.
5. It should be noted that all WC additions were accompanied by proportional reductions in total fiber content, meaning that the mechanical response reflects the combined effect of ceramic reinforcement and fiber removal; FESEM evidence confirms that agglomeration is the dominant factor at loadings above 15 wt%.

6. The 10–15 wt% WC range provides the best balance of fatigue resistance, hardness, and satisfactory static strength and represents the recommended design window for this hybrid system. These findings provide important reference data for the design of multi-functional hybrid composites for lightweight structural and protective applications.

Ethics Declaration

This study does not involve human participants, animals, or any biological samples. Accordingly, ethical approval and informed consent were not required. All references cited in the manuscript are appropriately acknowledged.

Funding Declaration

This research received no external funding.

Data Avail ability Statement

The data supporting the findings of this study are available from the corresponding author upon reasonable request.

CRediT authorship contribution statement

Deshmukh Dhiraj: Writing – review & editing, Supervision, Resources, Project administration, Investigation. **Nilesh Sitaram Gaikwad:** Methodology, Investigation, Formal analysis, Conceptualization.

Declaration of Competing Interest

The authors declare that they have no known competing financial interests or personal relationships that could have appeared to influence the work reported in this paper.

References

[1] E. Natarajan, T. Sekar, K. Markandan, et al., Structural integrity and mechanical behaviour of magnesium oxide (MgO) as reinforcement in PLA-HDPE composite, Emergent Mater. 7 (2024) 1283–1294, https://doi.org/10.1007/s42247-024-00650-z.
[2] S. Anidha, S. Mozhuguan Sekar, E. Natarajan, M. Muthukkumar, K. Markandan, C. K. Ang, G. Franz, Preliminary Investigations and Support for the Mechanical and Dynamic Characteristics of a Natural Rubber Reinforcement in E-Glass/CNT/Epoxy Composite, J. Compos. Sci. 8 (4) (2024) 140, https://doi.org/10.3390/jcs8040140.
[3] E. Natarajan, S. Mozhuguan Sekar, K. Markandan, C.K. Ang, G. Franz, Tailoring Basalt Fibers and E-Glass Fibers as Reinforcements for Increased Impact Resistance, J. Compos. Sci. 8 (4) (2024) 137, https://doi.org/10.3390/jcs8040137.
[4] E. Natarajan, L.I. Freitas, Santhosh, K. Markandan, A. a M. Al-Talib, C. Hassan, Experimental and numerical analysis on suitability of S-Glass-Carbon fiber reinforced polymer composites for submarine hull, Def. Technol. 19 (2022) 1–11, https://doi.org/10.1016/j.dt.2022.06.003.
[5] E. Natarajan, K. Markandan, S.M. Sekar, K. Varadaraju, S. Nesappan, A.D. Albert Selvaraj, W.H. Lim, G. Franz, Drilling-Induced Damages in Hybrid Carbon and Glass Fiber-Reinforced Composite Laminate and Optimized Drilling Parameters, J. Compos. Sci. 6 (10) (2022) 310, https://doi.org/10.3390/jcs6100310.
[6] Naik, N.K. (2016). Ballistic impact behavior of composites. 10.1016/B978-0-08-100080-9.00015-4.
[7] K. Ravikumar, K. Kiran, V.S. Sreebalaji, Characterization of mechanical properties of aluminium/tungsten carbide composites, Measurement 102 (2017) 142–149, https://doi.org/10.1016/j.measurement.2017.01.045.
[8] R. Shivashankar, G.V. Naveen Prakash, C. Manjunatha, V.B. Hemadri, K. M. Mrityunjaya Swamy, C.D. Prasad, K. Mahesh Dutt, Development and mechanical characterisation of hybrid tungsten carbide/graphite reinforced aluminium metal matrix composites using deep learning techniques, Can. Metall. Q. 65 (1) (2026) 334–349.
[9] V.N. Jawahar, R.J.H. Navasingh, K. Stebel, R. Jasiński, A. Niesłony, Improved Mechanical Performance of Carbon–Kevlar Hybrid Composites with TiO_2 Nanoparticle Reinforcement for Structural Applications, J. Manuf. Mater. Process. 9 (5) (2025) 140, https://doi.org/10.3390/jmmp9050140.
[10] T.G. Yashas, A. Vinod, P. Madhu, M.R. Sanjay, Suchart Siengchin, Mohammad Jawaid, Mechanical and thermal properties of flax/carbon/kevlar based epoxy hybrid composites, Polym. Compos. 43 (2022) 5649–5662, https://doi.org/10.1002/pc.26880.
[11] M. Rezasefat, Y. Kumar, A.A.X. da Silva, S.C. Amico, J.D. Hogan, A. Manes, Dynamic Behavior and Permanent Indentation in S2-Glass Woven Fabric Reinforced Polymer Composites under Impact: Experimentation and High-Fidelity Modeling, J. Compos. Sci. 8 (4) (2024) 138, https://doi.org/10.3390/jcs8040138.
[12] M. Mohammadi, E.M. Sosa, Enhancing mode-II delamination resistance of hybrid woven composite materials of glass/Kevlar fabrics by stitching with Kevlar threads, Compos. Struct. 345 (2024) 118365, https://doi.org/10.1016/j.compstruct.2024.118365.
[13] X. Jing, Y. Ding, S. Chen, F. Xie, A. Zhang, C. Zhang, Hybrid effects and failure mechanisms of S-glass/aramid fiber reinforced hybrid composite laminates with wave-transparent, Compos. Part. a Appl. Sci. Manuf. 197 (2025) 109036, https://doi.org/10.1016/j.compositesa.2025.109036.
[14] M.İ. Özsoy, M.Ö. Bora, S. Ürgün, S. Fidan, E. Güleç, Tribological Performance of Glass/Kevlar Hybrid Epoxy Composites: Effects of Pressurized Water-Immersion Aging Under Reciprocating Sliding Wear, Polymers 17 (21) (2025) 2944, https://doi.org/10.3390/polym17212944.
[15] K..S. Lokesh, D., S. Mayya, S. Shetty. S, K..C. V, G. R. B, H. G, H..L. Y, Thermo-mechanical performance of Kevlar based hybrid natural fiber composites pre-coated with termite modified epoxy polymer, Results Eng. 28 (2025) 107719, https://doi.org/10.1016/j.rineng.2025.107719.
[16] Tomasz Jankowiak, Amine Bendarma, Alexis Rusinek, Temperature Effects During Perforation of S2-Glass/Epoxy Composite Plates: Original Numerical Approaches and Comparison with Experiments, J. Dyn. Behav. Mater. 11 (2025), https://doi.org/10.1007/s40870-025-00474-w.
[17] A.C. Sayin, S. Danisman, E. Ersoy, C. Yilmaz, S. Kesriklioglu, Experimental and statistical damage analysis in milling of S2-glass fiber/epoxy and basalt fiber/epoxy composites, Polym. Compos. 45 (16) (2024) 15140–15158, https://doi.org/10.1002/pc.28826.
[18] H. Turkmen, R. Yıldız, Investigation of Fire Resistance and Thermal Wear Behavior of Chopped Basalt and Glass Fiber Reinforced Epoxy, Composites (2025), https://doi.org/10.21203/rs.3.rs-7715012/v1.
[19] N. Sapiai, A. Jumahat, N.A. Shamshulizam, M. Chalid, Effect of Angle Orientation and Fiber Hybridization on Impact Behaviour of Glass, Basalt and Arenga pinnata Composites, http://TUENGR.COM/V13/13A13R.pdf, Int. Trans. J. Eng. Manag. & Appl. Sci. & Technol. 13 (13) (2022) 1–13, https://doi.org/10.14456/ITJEMAST.2022.270.
[20] A.K. Hamzat, M.S. Murad, I.A. Adediran, et al., Fiber-reinforced composites for aerospace, energy, and marine applications: an insight into failure mechanisms under chemical, thermal, oxidative, and mechanical load conditions, Adv. Compos. Hybrid. Mater. 8 (2025) 152, https://doi.org/10.1007/s42114-024-01192-y.
[21] Alessandro Vescovini, Joziel Cruz, Dayou Ma, Chiara Colombo, Antonio Salerno, Otavio Bianchi, Sandro Amico, Andrea Manes, Experimental investigation on low-velocity impact behavior of glass, Kevlar, and hybrid composites with an elastomeric polyurethane matrix, Compos. Part. C Open. Access. 13 (2023) 100426, https://doi.org/10.1016/j.jcomc.2023.100426.
[22] S. Zhao, J. Huang, J. Cao, Y. Chen, X. Zuo, K. Yi, C. Zhang, Thickness effect on ballistic impact behavior of hybrid carbon/Kevlar composites, Compos. Sci. Technol. (2024).
[23] H. Jiang, X. Liu, S. Jiang, Y. Ren, Hybrid effects and interactive failure mechanisms of hybrid fiber composites under flexural loading: Carbon/Kevlar, carbon/glass, carbon/glass/Kevlar, Aerosp. Sci. Technol. 133 (2023) 108105, https://doi.org/10.1016/j.ast.2023.108105.
[24] Mahdi Hosseini, Milan Gaff, Petr Konvalinka, Hynek Maňák, Jensin Joshua, Ahmad Hosseini, Krishna Teja, S. Yogeswari, Pritam Ghosh, M. Chandrasekar, Kevlar/Basalt and Kevlar/Glass Intra-Ply Reinforced Hybrid Composites: Influence of Basket Weave Fabric Structure on Thermal Properties, Flammability, and Impact Performance, Macromol. Mater. Eng. 310 (2025), https://doi.org/10.1002/mame.202400391.
[25] E. Wakshume, S. Fanta, S. Seid, K. Yeneneh, Optimization of fiber-reinforced composites for lightweight ballistic body armour, Appl. Eng. Sci. 24 (2025) 100262, https://doi.org/10.1016/j.apples.2025.100262.
[26] A. Fajdek-Bieda, A. Wróblewska, The Use of Natural Minerals as Reinforcements in Mineral-Reinforced Polymers: A Review of Current Developments and Prospects, Polymers 16 (17) (2024) 2505, https://doi.org/10.3390/polym16172505.
[27] Koduru, Gagan & Bhavana, Munugapati & Thimmaraju, Pavan & Konda Reddy, Gondi & Esanakula, Jayakiran & Srividya, Ganja (2025). Mechanical properties and performance analysis of fiber-reinforced composite materials. 070043. ⟨10.1063/5.0297939⟩.
[28] Brian Bak, Carlos Sarrado, Albert Turon, Josep Costa, Delamination Under Fatigue Loads in Composite Laminates: A Review on the Observed Phenomenology and Computational Methods, Appl. Mech. Rev. 66 (2014) 060803, https://doi.org/10.1115/1.4027647.
[29] H. Ahmad, A.U.R. Shah, Mazullah, et al., Effect of Kevlar/Glass Hybrid Reinforcement on the Performance of Epoxy/Vinyl Ester Hybrid Resin, Polym. Compos. 47 (S1) (2026) S680–S690, https://doi.org/10.1002/pc.70830.
[30] M.Z. Hussain, S.Z.H. Shah, R.S. Choudhry, S.M. Hussnain, P.S.M. Megat-Yusoff, T. Sharif, S.B. Mahadzir, Fatigue life enhancement of fibre-reinforced composites: A state-of-the-art review and outlook, Results Eng. (2025) 108125.
[31] Z. Li, X. Chen, D. Liu, et al., Recent advances in polymer-based composites for thermal management and electromagnetic wave absorption, Adv. Compos. Hybrid. Mater. 8 (2025) 210, https://doi.org/10.1007/s42114-025-01243-y.
[32] Huan Tran, Chiho Kim, Rishi Gurnani, Oliver Hvidsten, Justin DeSimpliciis, Rampi Ramprasad, Karim Gadelrab, Charles Tuffile, Nicola Molinari, Daniil Kitchaev, Mordechai Kornbluth, Polymer Composites Informatics for Flammability, Thermal, Mechanical and Electrical Property Predictions, Polym. Chem. 16 (2025), https://doi.org/10.1039/D4PY01417K.

[33] Zhaoyang Li, Yu Sun, Feiyang Hu, Di Liu, Xiangping Zhang, Juanna Ren, Hua Guo, Marwan Shalash, Mukun He, Hua Hou, Salah El-Bahy, Duo Pan, Zeinhom El-Bahy, Zhanhu Guo, An overview of polymer-based thermally conductive functional materials, J. Mater. Sci. & Technol. (2024) 218, https://doi.org/10.1016/j.jmst.2024.07.053.

[34] Gaurish Vaze, Vedang Gogate, Mohit Lele, Ananya Sastry, Siddhant Amrutkar, Atharva Bapat, Vishal Salunkhe, Ballistic Impact Analysis of Carbon Fiber and E-glass Sandwiched Composites, Procedia Struct. Integr. 71 (2025) 395–400, https://doi.org/10.1016/j.prostr.2025.08.053.

[35] D.K. Singh, G. Tiwari, Ballistic impact behavior of laminated jute fiber structures against two projectile nose profiles, Mech. Res. Commun. 152 (2026) 104612, https://doi.org/10.1016/j.mechrescom.2026.104612.

[36] A. Biradar, S. Arulvel, J. Kandasamy, Significance of ballistic parameters and nanohybridization in the development of textile-based body armor: A review, Int. J. Impact Eng. 180 (2023) 104700, https://doi.org/10.1016/j.ijimpeng.2023.104700.

[37] R.F.P. Junio, B.S.A. de Cêa, D.S. Silva, É.P.L. Júnior, S.N. Monteiro, L. F. Nascimento, C, Computational and Experimental Ballistic Behavior of Epoxy Composites Reinforced with Carnauba Fibers: A Stand-Alone Target and Multilayered Armor System, Polymers 17 (4) (2025) 534, https://doi.org/10.3390/polym17040534.

[38] X. Lei, Xianqian Wu, Zhen Zhang, K. Xiao, Yiwei Wang, Chenguang Huang, A machine learning model for predicting the ballistic impact resistance of unidirectional fiber-reinforced composite plate, Sci. Rep. 11 (2021) 3, https://doi.org/10.1038/s41598-021-85963-.

[39] H. Fang, L. Xi, Y. Huang, T. Zhao, R. He, X. Kang, Y. Li, D. Fang, Fiber-reinforced composites: A comprehensive review of traditional and additive manufacturing processes and material architectures, Compos. Part. a Appl. Sci. Manuf. 205 (2026) 109684, https://doi.org/10.1016/j.compositesa.2026.109684.

[40] G. Jeevan, B. Kannan, R. Senthil, A comprehensive review of the performance, durability, and sustainability of natural and hybrid fiber-reinforced polymer composites, Compos. Part. B Eng. 323 (2026) 113800, https://doi.org/10.1016/j.compositesb.2026.113800.

[41] Amit Kumar, Saurav Dixit, Subhav Singh, S. Sreenivasa, Pardeep Bains, Rohit Sharma, Recent developments in the mechanical properties and recycling of fiber-reinforced polymer composites, Polym. Compos. 46 (2024) 3883–3908, https://doi.org/10.1002/pc.29261.

[42] Z. Kaya, H.E. Balcioglu, H. Gün, The strain rate and temperature effects on the static and dynamic properties of S2 glass/epoxy composites, Appl. Phys. A 126 (2020) 665, https://doi.org/10.1007/s00339-020-03855-1.

[43] S. Farajyar, H. Wan, Y. Wang, Finite element analysis of ballistic impact on Kevlar-29/epoxy composites with varying layer configurations, Int. J. Impact Eng. 208 (2025) 105538, https://doi.org/10.1016/j.ijimpeng.2025.105538.

[44] Tesfaye Worku, Challenges and Prospects of Composite Materials Manufacturing Using Textile Fibers as Reinforcement, Am. J. Mater. Synth. Process. 10 (2025) 1–5, https://doi.org/10.11648/j.ajmsp.20251001.11.

[45] P. Aghdasi, D.Y. Li, et al., Interfacial bonding between iron and Mo- and Cr-doped WC: A first-principles study, J. Appl. Phys. 133 (4) (2023) 045301, https://doi.org/10.1063/5.0134620.

[46] P. Aghdasi, D.Y. Li, et al., Work of adhesion analysis for metal-substituted W_4C_4 carbides in a cobalt matrix, Langmuir 39 (51) (2023) 18746–18756, https://doi.org/10.1021/acs.langmuir.3c02194.

[47] P. Aghdasi, D.Y. Li, Electron work function guided tailoring of $(W_{4x}, M_x)C_4$/doped Ni matrix interfacial bonding: Insights from first-principles calculations, Acta Mater. 283 (2025) 120511, https://doi.org/10.1016/j.actamat.2024.120511.